



14th IEA Heat Pump Conference
15-18 May 2023, Chicago, Illinois

An energetical, exergetical and experimental analysis of an absorption-heat exchanger used as transfer sub-station in an already existing district heating grid

Gerald Zotter^{a*}, Damian Eberhöfer^a, Carina Seidnitzer-Gallien^a

^aAEE INTEC; Feldgasse 19, Gleisdorf 82002, Austria

^bSecond affiliation, Address, City and Postcode, Country

Abstract

The application of an absorption-heat exchangers as transfer sub-station in a district heating grid can use the temperature difference between the primary (up to 145 °C) and secondary supply temperature (ca. 70 °C) of the circuits for subcooling the primary return temperature below the secondary one. This leads to the advantages of increased heat capacity within an existing grid up to 30% at unchanged flow and temperature inlet conditions on the one hand-side, and on the other hand-side, more renewables can be more easily integrated. To proof the required temperature gap between the two supply temperatures to ensure a subcooling of the primary return flow temperature below the secondary one has been experimentally investigated by a small pilot-scaled absorption-heat exchangers (about 10 kW max) at the laboratory of AEE INTEC at different inlet conditions. This analysis has shown that a subcooling up to 20.7 K is achievable between the return temperatures with an AHX at highly primary supply and low secondary return temperatures as long the mass flow of the secondary grid gets increased accordingly to the heat capacity increase.

© HPC2023.

Selection and/or peer-review under the responsibility of the organizers of the 14th IEA Heat Pump Conference 2023.

Keywords: heat exchanger effectiveness, transfer sub-station, exergy analysis, pinch point, renewables

1. Introduction

In Austria, more than about a quarter of the entire population and numerous companies are currently supplied of thermal energy by means of district heating (DH) [1], with a forecasted growing rate of 0.8%/anno in average for the next 5 years. This increasing demand is currently being covered by investments in network infrastructure and supply units. At the same time, however, a complete phase out of Gas (about 28% [1]) is limited by the fact that a considerable proportion of renewables and waste heat cannot be integrated in Austrians existing DH-grids based on not fitting temperature levels, which means that the temperature levels, particular in the so-called primary circuit is still too high. A further advantage of a reduction of the used supply temperature in the DH-Grid is the reduction of the distribution heat losses.

But for already existing heating networks - based on already installed pipelines, which means that the diameters of the pipes are also fixed - the maximum possible mass flow (\dot{m}) is limited and thus also the maximum possible heat capacity (\dot{Q}) of the network is limited, according to Eq. (1). The limitation of \dot{m} in existing pipes is based on cavitation avoidance reasons, where the flow velocity cannot be increased so that the local static pressure in the pipe does not fall below that of the saturation pressure. So, an increase of the heat capacity could be only achieved, if bigger pipes would be installed. But this creates high investment cost and long periods to refurbish the entire grid. To overcome this situation, the (primary) return temperature ($t_{R,Pr}$) has to be lowered by a higher value than the (primary) supply temperature ($t_{S,Pr}$), in order to achieve a bigger temperature-spread and thus ensure an increase of the heat capacity of the existing DH-grid, according to. With a sufficiently high reduction of the return temperature, the supply temperature could also be reduced

* Gerald Zotter. Tel.: +43 650 891 819 5

E-mail address: g.zotter@aee.at.

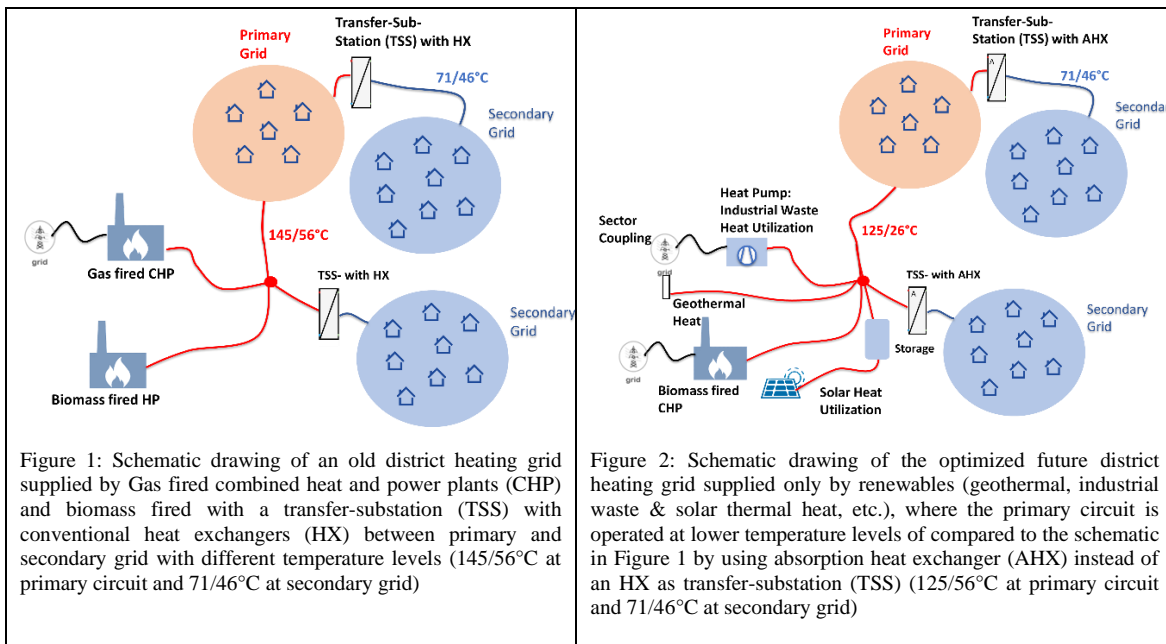
at a high value, which leads to a reduction of losses and significantly increases the possibility for the integration of renewables, such as deep geothermal or industrial waste heat (compare Figure 1 to Figure 2).

$$\dot{Q} = \dot{m} * c_p * (t_{s,Pr} - t_{r,Pr}) \quad (1)$$

Technologies such as electrically driven heat pumps and thermally absorption heat pumps (AHPs) are widely used to improve the overall efficiency of different energy supply systems in different applications [3-7]. The possibilities to use thermally-driven AHP in district heating and/or cooling grids are wide and cover a broad spectrum for increasing the energy efficiency. According to Hu et. al (2020) [8] the absorption heat exchanger (AHX) is one of the most commonly used technologies to improve performance of district heating grids. In comparison to a conventional heat exchanger (HX) an AHX can use the exergetic potential (second law of thermodynamics) based on the temperature difference between the supply temperatures ($\Delta t_{s,Pr/Se}$) (see Eq. 2) to sub-cool $t_{r,Pr}$ below the return temperature of the secondary circuit ($t_{r,Se}$), which is the inlet temperature of the on the secondary side of the TSS. This subcooling ($\Delta T_{Sub-R,Pr/Se}$, according to Eq.3) allows the improvement of the DH-grid, as already mentioned above, and the reason to use an AHX. A detailed explanation of the working principal of an AHX and a comparison to a HX are given in chapter **Error!**
Reference source not found..

$$\Delta T_{s,Pr/Se} = (t_{s,Pr} - t_{s,Se}) \quad (2)$$

$$\Delta T_{Sub-R,Pr/Se} = (t_{r,Se} - t_{r,Pr}) \quad (3)$$



So, using an AHX for transfer-sub-stations (TSS) instead of conventional heat exchangers (HX) are key for lowering the temperature levels of already existing DH-grids. Although, AHXs have a high potential for return flow temperature reduction of heating grids [9-10], those applications are still very rare in Austria. To overcome that situation, within this work a small pilot-scaled AHX (of about 10 kW, see Figure 10) has been experimentally investigated in detail at different boundary conditions at the laboratory of AEE INTEC.

2. Optimized transfer-sub-station

When a DH-grid is separated in circuits with different temperature levels (primary and secondary), the circuits are connected via TSS using conventional HX (see Figure 3). Generally, the temperature levels in the DH-grid depend on the ambient temperature. This is based on the fact that grid is operated by a weather-compensating control for the supply temperature, where minima supply temperatures have to be ensured

depending on a floating set value considering the weather conditions. For colder ambient conditions the supply temperature has to be higher than for warmer days. For the design point of about -10°C ambient temperature the supply/return temperature in the primary grid is about 145°C/58°C, where else on the secondary grid it is about 70°C/45°C.

2.1. Using heat exchanger as TSS

As mentioned in chapter 1, from an energetical point of view the primary return temperature should be as low as possible. The primary return temperature depends at that case on the arrangement of the HX (parallel- or counter-flow) and the so-called pinch-point temperature difference (Δt_{pp}). Δt_{pp} is influenced by the heat transmission coefficient (U) and the heat transfer area of the HX (A). This means for example that an increase of A of about 40% (see Figure 3 and Figure 5) could lower Δt_{pp} to the half and this raises \dot{Q} of about 7% at constant inlet conditions, as shown by a comparison of the two t vs \dot{Q} - diagram in Figure 4 and Figure 6.

Even if, the heat exchanger efficiency (η , see Eq. 5) is mostly 100% as long as the heat losses (\dot{Q}_{loss}) are neglectable, but a change of Δt_{pp} has an influence on the heat exchanger effectiveness (ϵ , see Eq. 4) as well as different inlet conditions concerning \dot{m} , c_p and temperature. Based on the conditions shown in Figure 4 the HX has an ϵ of 0.9, where else the HX with the increased A has an effectiveness of 0.95.

$$\epsilon = \frac{\text{actual heat transfer}}{\text{maximal possible heat transfer}} = \frac{\dot{m}_{Pr} * c_{p,Pr} * (t_{S,Pr} - t_{R,Pr})}{|\dot{m} * c_p|_{min} * (t_{S,Pr} - t_{R,Se})} \quad (4)$$

$$\eta = \frac{\dot{Q}_{Pr} (-\dot{Q}_{loss})}{\dot{Q}_{Se}} \quad (5)$$

2.2. Using absorption heat exchanger as TSS

A (single-stage) AHP is driven by heat and consists of an evaporator, where heat gets absorbed from a cold heat source (cold water). The vaporized refrigerant flows to the absorber, where the solution fluid absorbs the refrigerant by rejecting heat to a mid-temperature heat sink (cooling water). The (refrigerant) rich solution gets pumped over the solution HX (where sensible heat between the hotter poor solution and colder rich solution is transferred) into the generator. The generator gets driven by heat from the hot heat source (hot water) to desorb the refrigerant from the solution. The poor solution flows via a throttle and the solution HX back to the absorber, where else the refrigerant flows to the condenser. The condenser rejects latent heat to the mid-temperature heat source to fully condensate the refrigerant. The condensate gets expanded via another throttle to the evaporator. Evaporator and absorber operate (if pressure losses could be neglected) at the same low-pressure level. Condenser and generator operate (if pressure losses could be neglected) at the same high-pressure level.

The AHX is a combination of an absorption chiller with an HX, as shown Figure 7, which is not used as a chiller or heat pump, but as an energetically optimized HX. As though, the hot water- (external heat transfer fluid-circuit) is short-circuited with the cold water-circuit (external heat transfer fluid-circuit) of the absorption chiller via the heat exchanger; this side represents the primary circuit of the AHX. For the secondary side, the cooling water (external heat transfer fluid-circuit) gets partitioned between the HX and the absorber chiller via the distribution valve (D-valve).

2.3. Analysis of TSS based on the second law of thermodynamics

The AHX is using the exergetic potential (ex_{pot}) of the otherwise unused big temperature gap between the two supply temperatures ($\Delta t_{S,Pr/Se}$) to drive an AHP for subcooling $t_{R,Pr}$ below $t_{R,Se}$ in the evaporator of the AHP. At the given boundary conditions, according to Figure 6, the HX offers a theoretical ex_{pot} of ca. 15% ($T_a = 293.15$ K) which could be used to operate an AHX (according to Eq. 6), but would be irreversibly wasted in a conventional HX. That potential is shrinking to zero when $\Delta t_{S,Pr/Se}$ is decreasing to zero: However, this is a theoretical potential not covering the temperature glides, pressure losses, irreversibility in each single heat exchanger etc. is not covered. However, as shown in Figure 8, which is based on an OD simulation model in EES [13] a subcooling ($\Delta t_{Sub-R,Pr/Se}$) of 21 K can be achieved by a first principal model, with $\Delta t_{pp} > 3$ K in every single heat exchanger of the AHX. According to that, see Figure 8, the heat capacity

could be increased of about 30%, in which the secondary mass flow has to be increased also of the same 30% that the surplus of \dot{Q} could be transferred without raising $t_{s,se}$. This is required to avoid that the ex_{pot} would not be lowered, which is required to drive the AHX.

Furthermore, a detailed exergy analysis - based on the Gouy-Stodola-Equation, considering the different entropy changes (see Eq. 7) on primary ($\dot{m}_{pr} * \Delta s_{ps}$) and secondary ($\dot{m}_{se} * \Delta s_{se}$) side - shows irreversible exergy losses within the HX and AHX. This analysis shows that up to 30% of the irreversibility can be reduced using an AHX compared to an HX (neglecting the pumps and each single pinch point temperature difference from generator to evaporator). Within this exergetical improvement the AHX could achieve an ϵ of 1.15. This is only possible due to counter-clockwise rotated cycle is used within the AHX and the driving source comes from the otherwise unused exergetical potential, as already mentioned. However, the exergetical efficiency of the AHX is of course still below 1 and amounts to 0.93 for the boundary conditions listed in table 1.

$$ex_{pot} = \frac{\dot{Ex}}{\dot{Q}} = T_a \frac{(T_{s,pr} - T_{s,se})}{(T_{s,pr} * T_{s,se})} \quad (6)$$

$$-\frac{dEx_{Irr}}{d\tau} = T_a * [\sum \dot{m}_{se} * s_{se} - \sum \dot{m}_{pr} * s_{pr}] \quad (7)$$

$$\eta_{ex} = \frac{Ex_{in} - Ex_{irr}}{\dot{Q} Ex_{in}} \quad (8)$$

Table 1. A comparison of the boundaries and efficiencies/effectiveness for HX and AHX

Transfer-sub-station using	$t_{s,pr}$ (°C)	$t_{r,pr}$ (°C)	\dot{m}_{pr} (kg/s)	$t_{s,se}$ (°C)	$t_{r,se}$ (°C)	\dot{m}_{se} (kg/s)	\dot{Q} (MW)	ϵ -	η_{ex} -
HX	145	52	16.1	71	46	62.5	6.3	0.95	0.91
AHX	145	25	16.1	71	46	77.4	8.1	1.15	0.93

According to Figure 8, the exergetical benefit of an AHX is that the high temperature level of the supply-side of the primary circuit is used to drive the generator, where that high temperature level is required. All pinch point temperature in the AHX is positive. The directly sub-cooling ($\Delta T_{sub-r,pr/se}$) happens in the evaporator of the AHX. To count the energetical potential of an AHX not only $\Delta T_{sub-r,pr/se}$ should be considered, but also the pinch point temperature difference which is required for a conventional HX. This means that the entire temperature difference between the primary return temperature of a HX and an AHX is in that particular case 27 K (compare Figure 5 to Figure 7).

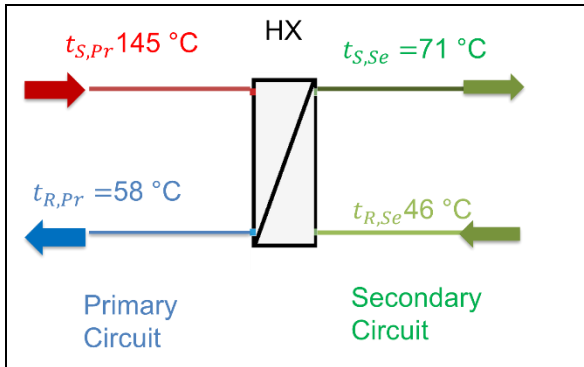


Figure 3: Principal picture of a conventional heat exchanger (HX) used as transfer sub-station (TSS) in a district heating grid (DH) including temperature levels of external heat transfer fluids of primary and secondary site

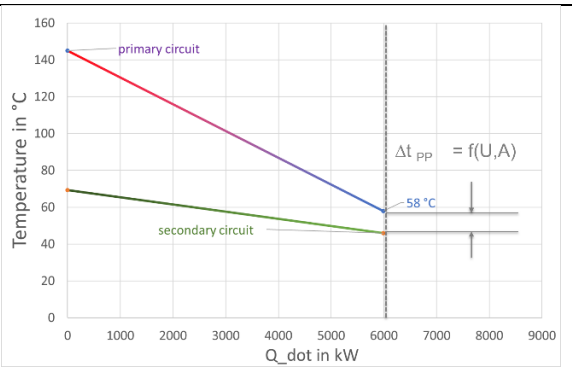


Figure 4: Pinch point temperature difference (Δt_{pp}) in the temperature vs. heat capacity – diagram (t vs. \dot{Q} – diagram) of a transfer sub-station

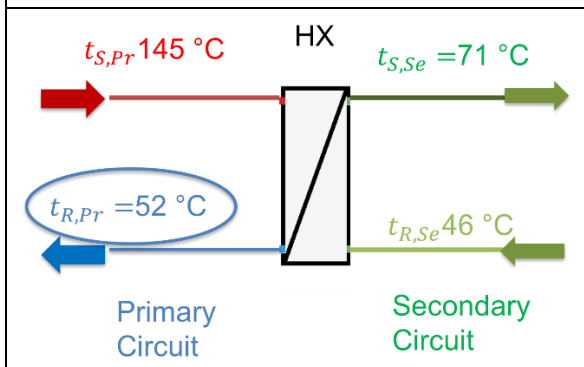


Figure 5: Principal picture of a conventional HX used as TSS in a DH-grid including temperature levels of external heat transfer fluids of primary and secondary site with 40% bigger heat transfer area (A) compared to Figure 3

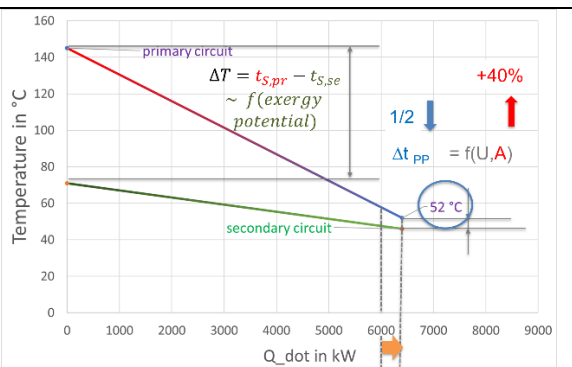


Figure 6: t vs. \dot{Q} – diagram of a 40% bigger HX compared to Figure 5 lowering Δt_{pp} to the half and increasing \dot{Q} of about 7%; furthermore, also the big temperature difference between the supply temperature of the primary circuit

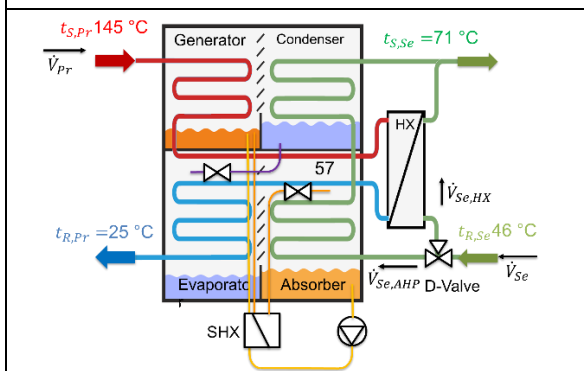


Figure 7: Principal picture of an absorption heat exchanger (AHX) consisting of an AHP and a HX and a distribution valve (D-valve)

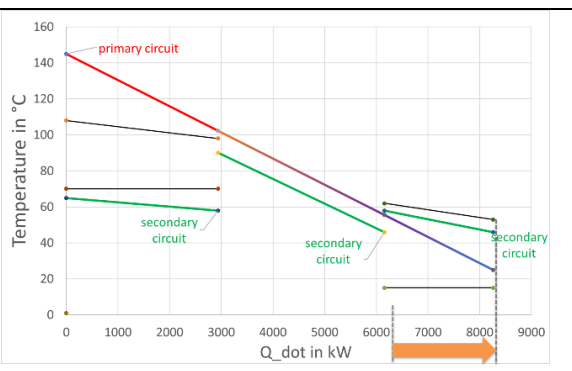


Figure 8: t vs. \dot{Q} – diagram of all heat exchangers of an AHX and an increased \dot{Q} of about 30%; furthermore,

From a thermodynamical point of view, an AHX can be seen as a combination of a Rankine cycle and compression chiller, as shown in Figure 9. The supply side of the primary circuit is used as heat sink of the Rankine cycle and the supply side of the secondary circuit is used as its heat sink. The electrical power produced by a Rankine cycle is used to drive a Perkins/Evans cycle, where the return-side of the secondary circuit is used as heat sink and the return-side of the primary circuit is used as heat source. So, an AHX is a combination of a HX and a clockwise- and counterclockwise rotating thermodynamical cycles, where exergy fluxes are used regarding its temperature levels.

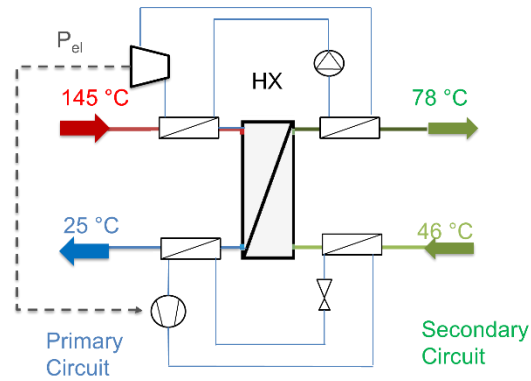


Figure 9: Principal drawing of a combination of a Rankine Cycle and a Perkin/Evans Cycle to sub-cool the return temperature below the one of the

3. Test bench of the pilot-scaled AHX

Within this work a pilot-scaled AHX was designed and set up as a combination of an AHP (absorption chiller: single-stage chiller with solution HX, available on the market with a nominal cooling capacity of 15 kW, see Figure 9 in orange) and a plate-HX (see Figure 9 in green, with A of 2.46 m²), in a counterflow arrangement. The working pair used in the AHP was water/Lithium-Bromide (H₂O-LiBr). As shown in Figure 10, the AHX been equipped with the required measurement equipment and integrated into the infrastructure of the laboratory of the AEE INTEC (blue-marked) consists of a heat-sink/-source system, and analyzed at different operating conditions. For that, the primary inlet (“supply”) and the secondary inlet (“return”) temperature and as well as volume flow ratio between primary and secondary site has been varied, as well as the secondary distribution ratio (see table 2). All energy fluxes have been measured at internal AHX cycle as well as on the external primary and secondary circuits. After calibration of the measurement equipment the uncertainties of the temperature sensors amount only ± 0.2 K, of the volume flow meter only about ± 0.5% of the measured value.

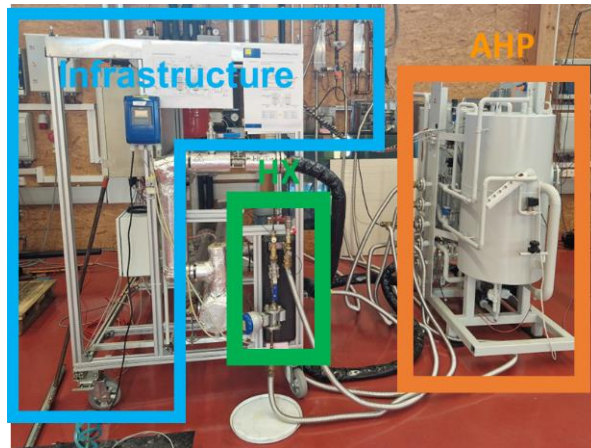


Figure 10: Picture of the AHX test bench at AEE INTEC, consist of an AHP (in orange) and a HX (in green) integrated in the infrastructure of the laboratory

At that point it has to be mentioned, that regarding safety reasons thermo-oil was used as heat transfer fluid for the primary side instead of pressurized hot water (up to 20 bar, avoiding cavitation for 145 °C). This had in influence on lowering the possible heat capacity of the tested AHX down to max. 10 kW. Particularly, the differences between heat transfer coefficients (HTC) and specific heat capacities (c_{ps}) of the two fluids must be taken into account. In addition, the energy balance was drawn for stationary points and the corresponding heat losses were analyzed, see. The convective and radiative heat losses were evident (of about 10%) due to the lack of thermal insulation, but could be balanced out for the analysis.

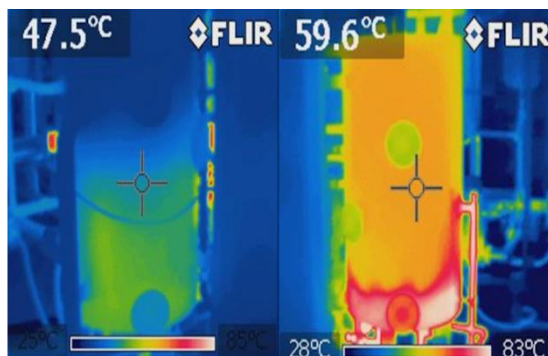


Figure 11: Infrared photograph of the evaporator-absorber reactor (left) and the condenser-generator reactor (right); to determine the heat losses [14]

However, to simplify the data collection parameter for the ratios of volume flows, as mentioned above, has been determined. So, the ration of volume flows between primary and

secondary circuit is called general volume flow ratio (GVR, see Eq. 9)- and the ratio between the secondary volume flow through the HX and the AHP is called secondary volume flow ratio (SVR, see Eq.9)

$$GVR = \frac{\dot{V}_{Se}}{\dot{V}_{Pr}} \quad (9)$$

$$SVR = \frac{\dot{V}_{Se,HX}}{\dot{V}_{Se,AHX}} \quad (9)$$

Table 2. Parameter (and values) for measurement matrix of AHX

Name of parameter	Values	Measurement uncertainties
$t_{S,Pr}$ in °C	145, 125, 105	± 0.2 K
$t_{R,Se}$ in °C	38, 44, 50, 56	± 0.2 K
\dot{V}_{Pr} in m ³ /h	250	± 0.5% of the measured value
GVR in -	3, 4.5, 6	$\pm \sqrt{\left(\left(\frac{\pm 0.5\%MVSE}{\pm 0.5\%MVPR}\right)^2 + \left(\frac{\pm 0.5\%MVPR}{\pm 0.5\%MVPR}\right)^2\right)}$
SVR in -	2, 0.5, 0.2	$\pm \sqrt{\left(\left(\frac{\pm 0.5\%MVHX}{\pm 0.5\%MVHRP}\right)^2 + \left(\frac{\pm 0.5\%MVHRP}{\pm 0.5\%MVHX}\right)^2\right)}$

4. The measurement results

Within this experimental analysis the maximal possible subcooling ($t_{R,Se} - t_{R,PR}$) within the pilot-scaled AHX has been investigated in detail, according given boundaries in table 2. Covering all the different variants by changing that parameter as shown in table 2, the measurement matrix consists of 36 different measurement points. Each individual measurement point was recorded dynamically and when the external temperatures and volume flows as well as the internal (high and low) pressure levels settled to a stable asymptote, the steady state was evaluated. In those experimental investigations, the transient behavior of the AHX was also determined, but this is not the subject of this paper.

Figure 12 shows the subcooling of the primary return temperature below the secondary one ($t_{R,Se} - t_{R,PR}$) depending on primary supply temperature at different $t_{R,Se}$ and constant \dot{V}_{Pr} of 250 m³/h; GVR of 4.5 and a SVR of 0.2. The highest ($t_{R,Se} - t_{R,PR}$) can be achieved at high supply temperatures on the primary circuit and low return temperatures of the secondary circuit. However, high ($t_{R,Se} - t_{R,PR}$) has been measured also at higher $t_{R,Se}$ up to 56 °C, as long as $t_{S,Pr}$ is high. Furthermore, even at a low $t_{S,Pr}$ of 105 °C a sub-cooling of about 12 K could be measured as long as $t_{R,Se}$ is not warmer than 44 °C. No sub-cooling could be achieved at low $t_{S,Pr}$ and high $t_{R,Se}$.

Figure 14 shows the subcooling of the primary return temperature below the secondary one ($t_{R,Se} - t_{R,PR}$) depending on GVR at different SVR and constant \dot{V}_{Pr} of 250 m³/h; $t_{R,Se}$ of 44°C. For higher sub-cooling the ratio between volume flow rate of the secondary circuit to the one of the primary circuits has to be high. The same is valid for the SVR, as shown in the Figure 13. Figure 13 shows the sub-cooling of the primary return temperature below the secondary one ($t_{R,Se} - t_{R,PR}$) depending on SVR at different $t_{R,Se}$ and constant \dot{V}_{Pr} of 250 m³/h and GVR of 6. As more volume flow rate passes the AHP as higher is the sub-cooling. There is a limitation based on the required pump power and on the heat which has to be transferred of the HX to cool down the primary circuit coming from the generator and before entering the evaporator. Furthermore, within this investigation room for improvements has been detected regarding thermal insulation of the AHP, the internal control of the solution pump and the throttles, as well as on changes by the cycle of the AHP itself, like connecting the absorber and the condenser not in a serial but in a parallel arrangement.

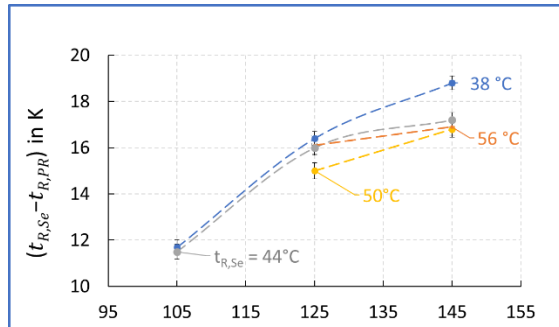


Figure 12: Subcooling of the primary return temperature below the secondary one ($t_{R,Se} - t_{R,PR}$) depending on primary supply temperature at different $t_{R,Se}$ and constant $\dot{V}_{Pr} = 250$ m³/sh; GVR =4.5, SVR = 0.2

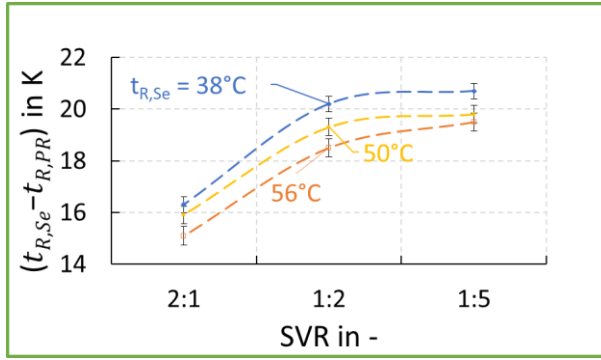


Figure 13: Subcooling of the primary return temperature below the secondary one ($t_{R,Se} - t_{R,PR}$) depending on SVR at different $t_{R,Se}$ and constant $\dot{V}_{pr} = 250 \text{ m}^3/\text{h}$ and GVR of 6

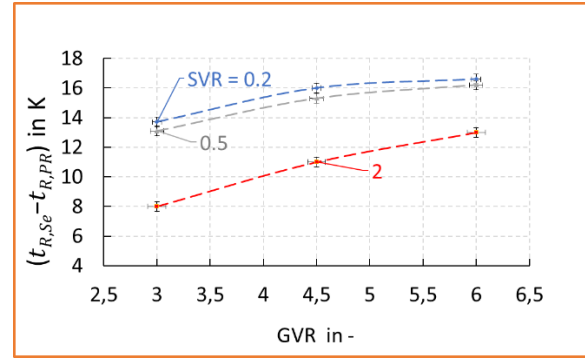


Figure 14: Subcooling of the primary return temperature below the secondary one ($t_{R,Se} - t_{R,PR}$) depending on GVR at different SVRs and constant $\dot{V}_{pr} = 250 \text{ m}^3/\text{h}$; $t_{R,Se} = 44^\circ\text{C}$

5. Conclusions

The application of an AHX as a TSS in a DH-grid can use the temperature difference between the primary (up to 145°C) and secondary supply temperature (ca. 70°C) of the circuits for subcooling the primary return temperature below the secondary one. This leads to the advantages of increased heat capacity within an existing grid up to 30% at unchanged flow and temperature inlet conditions on the one hand-side, and on the other hand-side, more renewables can be more easily integrated. As shown in this work, this is based on the fact that the exergy losses could be reduced by about 30% compared to a conventional HX and the heat capacity could be extended of about 30%. Furthermore, an AHX offers that the heat exchanger effectiveness could be increased to 115%, but the exergetical efficiency is of course still below 1 (0.94 at the same boundary conditions). However, this exergetical potential for optimization depends on the difference between the supply temperatures of the primary and secondary circuit. If the supply temperature of the primary circuit is close to the one of the secondary side no driving potential for subcooling the return temperature is available.

Considering that, within this work an experimental investigation of an AHX was covered and described in order to analyze its performance as a TSS being considered in DH-grids. The main focus was on the subcooling performance of the return temperature of primary circuit influenced by the difference between the supply temperatures of the primary and secondary circuits. For this research, an AHX at pilot-scale was designed, consist on a $\text{H}_2\text{O-LiBr}$ - absorption chiller, available on the market (nominal cooling capacity of 15 kW) and the plate heat exchanger with a heat transfer Area of (2.46 m^2) and integrated in the test facility of the laboratory of AEE INTEC. The test rig was driven by various temperature and mass flow inlet parameter variations in order to analyze the optimal operating points, the limitation for subcooling based on the minimal required difference between the supply temperature on steady-state points as well as to investigate the transient behavior of the AHX and explore a fitting control strategy regarding the mass flow distribution. Energy balancing was also carried out to determine the heat losses or inputs from the ambience.

The results of the experimental measurement series show that a high primary supply temperature, a low secondary return temperature and a high secondary-to-primary mass flow rate are required for a high subcooling performance. The partitioning of the secondary mass flow between the absorption chiller and the heat exchanger also had an effective effect, with a high mass flow through the chiller increasing subcooling. At $t_{s,Pr}$ of 145°C and $t_{R,Se}$ of 38°C , a SVR of 0.2 and GVR of 6 the highest subcooling with 20.7K could be achieved within the pilot scaled AHX. But even under suboptimal conditions, like low primary supply temperatures of 105°C the AHX subcooled the primary return temperature below the secondary of 12.4K, but for that a low return temperature on the secondary side below 44°C is required. For $t_{R,Se}$ higher than 50°C a minimal $t_{s,Pr}$ of 125°C is required.

Furthermore, the measurements have underlined the theoretical considerations about the exergetical driving potential that can be used by the AHX. Namely a big difference between the supply temperatures between primary and secondary circuit is required to sub-cool the return temperature at its most. This means that, for a constant mass flow of the primary circuit, the temperature spread has to increase by raising heat capacity of the AHX. Therefore, the mass flow on the secondary side must also be increased so that the heat capacity can be increased without increasing the supply temperature on the secondary circuit, that the exergetical driving potential stays constant. So at higher GVR a higher sub-cooling ($\Delta T_{\text{Sub-R,Pr/Se}}$) could be achieved within the

AHX. In addition, a distribution valve is needed on the secondary side so split the secondary volume flow between a part which flows through the AHP and through the HX (SVR). This experimental investigation shows that if more volume flow rate flows through the AHP part of the AHX the sub-cooling ($\Delta T_{\text{Sub-R,Pr/Se}}$) raises.

In conclusion, an AHX have high potential avoiding exergetical losses in a transfer-sub-station of a DH-grid and therefore the heat capacity in existing DH-grids could be increased, particular if renewables like deep geothermal heat or solar heat is used for suppling it.

6. Outlook

The experimental investigation of an AHX shows a high potential for reducing the primary return temperature of district heating networks and thus also a high replication potential for other substations, which can thus contribute to the increased use of exclusively renewable energy sources in DH-grids in Austria and Europe. This potential is based on the reduction of the return temperature, as this can also reduce the flow temperature, and thus renewable such as 'deep geothermal energy, solar thermal energy' and regenerative such as waste heat can be integrated much more efficiently into the grid. However, a necessary reduction of the flow and return temperatures on the secondary side must also be provided.

However, a necessary reduction of the flow and return temperatures on the secondary side must also be provided. Ergo, suitable measures must also be provided for the end user, such as for example surface heating, building mass activations, sufficiently large house transfer stations, etc.

But before that, from a technical point of view, it is important to convert results that are partly related to thermal-oil, which was used as heat transfer fluid for the primary side should be transferred to pressurized hot water. The measured values have to be transformed considering the higher c_p and HTC of water compared to thermo-oil on the primary side. Before the AHX is used in full-scale as a transfer substation, an optimized flow-layout, such as parallel connection of condenser and absorber, use of a multi-chamber machine and a corresponding control strategy for the distribution between secondary mass flow by the absorption machine part and the heat exchanger part has to be investigated in detail.

From an economical point of view, a further dynamic year-round simulation is essential for the economic evaluation in order to determine by how much the primary return can be supercooled. However, the economic consideration also requires a precise analysis of the supply side used. Especially renewables such as geothermal energy are extremely interesting; because by lowering the return temperature at the same flow rate, more heat can be drawn from this regenerative source free of charge. But, also the bigger packing and the issue with the required space of an AHX has to be considered. A planned demonstration of this integration concept of an AHX into a DH-grid shows high replication potential for other TSS, which can therefore contribute to the increased market penetration of these systems in Austria and Europe.

Acknowledgements

This work has been carried out within the project “AbSolut” (FFG-Nr.: 879433), which was financially supported by the “Klima und Energiefonds” within the national research program “Vorzeigeregion Energie” by the Austrian research funding association “FFG”. The authors also wish to thank the project partners, “WIEN ENERGIE GmbH”, “StepsAhead Energiesysteme GmbH”, “LINZ STROM GASWÄRME GmbH”, “EQUANS Energie GmbH” for their support and contributions.

Nomenclature

A	heat transfer area of the heat exchanger	$t_{S,Pr}$	primary supply temperature
AHP	absorption heat pump	$t_{S,Se}$	secondary supply temperature
AHP	absorption heat exchanger	U	heat transmission coefficient
COP	coefficient of performance	\dot{V}	volume flow rate
c_p	(isobaric) specific heat capacity	\dot{V}_{Pr}	volume flow rate on the primary circuit
DH	district heating	\dot{V}_{Se}	volume flow rate on the secondary circuit
D-valve	distribution valve	$\dot{V}_{Se,HX}$	volume flow rate through HX on the secondary circuit
EER	energy efficiency ratio	$\dot{V}_{Se,AHP}$	volume flow rate through AHP on the secondary circuit
Ex	exergy flux	TSS	transfer-sub-stations
ex_{pot}	exergetica potential		
\dot{E}_x	exergy flux		

$\dot{E}x_{trr}$	exergy losses	s	entropy
GVR	general volume flow ratio	SVR	secondary volume flow ratios
HTC	heat transfer coefficient	ΔT_{PP}	pinch-point temperature difference
\dot{m}	mass flow rate	$\Delta T_{S,Pr/Se}$	difference of supply temperatures
\dot{Q}	heat capacity, heat flux	$\Delta T_{Sub-R,Pr/Se}$	subcooling: difference between secondary and primary return temperature
\dot{Q}_{Pr}	heat flux emitted from the primary circuit	ΔS_{Pr}	entropy change on the primary side
\dot{Q}_{Se}	heat flux absorbed to the secondary circuit	ΔS_{Se}	entropy change on the secondary side
T, t	temperature (K, °C)	ϵ	heat exchanger effectiveness
T_a	ambient temperature	η	heat exchanger efficiency
$t_{R,Pr}$	primary return temperature	η_{ex}	exergetical efficiency
$t_{R,Se}$	secondary return temperature		

References

- [1] Federal Ministry for Climate Protection, Environment, Energy, Mobility, Innovation and Technology (BMK), 2020: Energy in Austria Figures, data, facts, Vienna, in German: Bundesministerium für Klimaschutz, Umwelt, Energie, Mobilität, Innovation und Technologie (BMK), 2020: Energie in Österreich Zahlen, Daten, Fakten, Wien, <https://www.bmk.gv.at/themen/energie/publikationen/zahlen.html>
- [2] Zotter, G, Seidnitzer-Gallien, C., Eberhöfer, D. (2022) Analysis of an absorption-heat exchangers used as transfer sub-station in a district heating grid based on the first and second law of thermodynamics Poster Contribution at EuroSun 2022: ISES and IEA SHC Conference on Solar Energy for Buildings and Industry, 25 - 29 September 2022, Kassel
- [3] Altenkirch E., 1954: „Absorptionskältemaschinen“, VEB Verlag Technik, Berlin
- [4] Bosnjakovic F. 1960. „Technische Thermodynamik, II. Teil“, 3. Auflage, in Wärmelehre und Wärmewirtschaft in Einzeldarstellungen (Band 12), Verlag von Theodor Steinkopff Dresden und Leipzig, p. 222 – 244
- [5] Radermacher R., Ling J., Gluesenkamp K. 2013. „Design of a Combined Cooling, Heating and Power Unit driven by IC Engine“, in Proc. *Deutsche Kälte-Klimatagung 2013*, Hannover, Deutscher Kälte-Klimatechnischer Verein (DKV), Band 4, ISBN 978-3-932715-49-5
- [6] Ziegler F. 2002: “State of the art in sorption heat pumping and cooling technologies” *International Journal of Refrigeration*, Vol. 25/4, 06.2002, pp. 450-459
- [7] Zotter, G., Rieberer, R., 2014: Increasing energy efficiency in Austrian industry through internal waste heat utilization by means of heat pump systems using two examples (in German) – Proc. Paper @ 13. *Symposium Energieinnovation*, 12.-14.2.2014, Graz/Austria
- [8] Hu, J., Xie, X., Jiang, Yi, 2020: Design and experimental study of a second type absorption heat exchanger: *International Journal of Refrigeration* 118 (2020) 50–60
- [9] Fu, L., Li, Y., Zhang, S., & Jiang, Y. (2010). A district heating system based on absorption heat exchange with CHP systems. *Frontiers of Energy and Power Engineering in China*, 4(1), 77–83. <https://doi.org/10.1007/s11708-010-0022-0>
- [10] Li, Y., Fu, L., Zhang, Sh., Jiang, Y., Xiling, Z., 2011: A new type of district heating method with co-generation based on absorption heat exchange (co-ah cycle) - *Energy Conversion and Management* 52 (2011) 1200–1207
- [11] Li Zhu, C., Xie, X., Jiang, Y., 2016: A multi-section vertical absorption heat exchanger for district heating systems - *International Journal of Refrigeration* 71 (2016) 69–84
- [12] Zotter, G., Rieberer, R., 2014: Increasing energy efficiency in Austrian industry through internal waste heat utilization by means of heat pump systems using two examples (in German) – Proc. Paper @ 13. *Symposium Energieinnovation*, 12.-14.2.2014, Graz/Austria
- [13] EES 2010. “Engineering Equation Solver”, © 1992-2010 S.A. Klein, Academic Professional V8.659-3D (09/1/10), F-Chart Software, Madison, Wisconsin